Few-Body Syst (2013) 54:685–695
DOI 10.1007/s00601-012-0443-x

Nils Elander · Sergei Rakityansky

Resonances and Their Relations to Spectral Densities and Scattering Cross Sections in the Schrödinger Formulation

Received: 12 March 2012 / Accepted: 6 April 2012 / Published online: 27 April 2012

Abstract The concept of resonances for a two-body single and many channel Schrödinger problem is discussed with respect to the Titchmarsh–Weyl theory. It is argued that the contributions from the entire set of resonances together with the free particle spectral density build the entire spectrum. The implication of this statement on the influence of resonances on a two-body scattering cross section is discussed. It is described how the residues of the S-matrix at a complex resonance energy, i.e. two complex numbers, is used to define its contribution to the cross section. The limitations of the Breit–Wigner approximation is discussed.

1 Introduction

Structures in scattering cross sections and decaying quantum states and the time development of quantum systems are subjects which are commonly discussed in modern few-body physics in general and at the workshop on Critical Stability in Erice, 2011. In this contribution we have therefore chosen to give a review of some of our earlier work to relate the definitions of the rigorous resonance concept, in the Aguilar–Balslev–Combes–Simon sense and discuss the influence of resonances, in a wide sense, to the spectrum of a two-body Schrödinger problem in potential scattering. In order to get an understanding of how the set of bound states and resonances are connected to a a set of potential energy curves we will consider two related approaches.

First we will review the Titchmarsh–Weyl theory and its relations to spectral densities. This part is intended to present an understanding of how the bound and continuous spectrum can be decomposed into contributions from the set of discrete eigenvalues of the Schrödinger problem.

Then we will turn to S-matrix theory and review work on the influence of resonances on scattering cross sections. Finally we will summarize and connect the approaches and point out some general conclusions.

2 Titchmarsh–Weyl Theory and Its Relation to Spectral Densities

When asking a mathematician about the continuous spectrum of a Schrödinger operator they may refer you to the classical book of Coddington and Levinsson [1] where the authors, in chapter 9, extends the theory of

N. Elander (✉)
Molecular Physics Division, AlbaNova University Center,
Stockholm University, 106 91 Stockholm, Sweden
E-mail: elander@fysik.su.se
Tel.: +46-8-55378656
Fax: +46-8-55378601

S. Rakityansky
Department of Physics, University of Pretoria, Pretoria 002, South Africa
E-mail: rakitsa@up.ac.za

self-adjoint two-body eigenvalue problems on a finite interval to a boundary-value problems for second-order differential equations.

2.1 The Schrödinger Equation and the Green Function

Let us therefore state the problem as was described in ref. [2]. Consider first the Schrödinger partial wave eigenvalue problem

$$L_\ell u(r) = \lambda u(r) \quad \text{with } L_\ell = -\frac{d^2}{dr^2} + \frac{\ell(\ell+1)}{r^2} + V_0(r) \tag{1}$$

It is related to the Green function

$$(\lambda - L_\ell) G_\ell^+(r, r') = \delta(r - r') \tag{2}$$

Let now $\psi_\ell(r)$ be the regular Schrödinger solution as $r \to 0$ and $\chi_\ell(r)$ be the regular Schrödinger solution as $r \to \infty$. Since for a fixed r' the Green function is regular as $r \to 0$ and $r \to \infty$ we have

$$G_\ell^+(r, r') \propto \psi_\ell(r) \quad \text{when } r \to 0 \quad \text{and} \quad G_\ell^+(r, r') \propto \chi_\ell(r) \quad \text{when } r \to \infty \tag{3}$$

$$\Rightarrow \quad G_\ell^+(r, r') = \psi_\ell(r_<)\chi_\ell(r_>)/W[\psi_\ell, \chi_\ell]. \tag{4}$$

2.2 The Classical Titchmarsh–Weyl Theory

The classical Titchmarsh–Weyl theory starts by considering the one-dimensional partial wave Schrödinger Eq. (1) on a finite interval $[0, b]$ and let ϕ_ℓ and ψ_ℓ be two linearly independent solutions at a given eigenvalue λ. They are then defined through

$$\begin{pmatrix} \phi_\ell & \psi_\ell \\ \phi'_\ell & \psi'_\ell \end{pmatrix}_{r=a} = \begin{pmatrix} \sin\alpha & \cos\alpha \\ -\cos\alpha & \sin\alpha \end{pmatrix} \text{ where } a \in (0, b) \tag{5}$$

Any Schrödinger solution, except ψ_ℓ, can then be written as:

$$\chi_\ell(r) = \phi_\ell(r) + \psi_\ell(r) m(E) \tag{6}$$

This equation defines the Titchmarsh–Weyl m-function. Now impose the boundary condition at $r = b > a$

$$\cos(\beta)\chi_\ell(b) + \sin(\beta)\chi'_\ell(b) = 0; \quad -\pi \le \beta \le \pi \tag{7}$$

Using the fact that $\beta \in \mathrm{R}$ implies

$$\mathcal{I}m(\chi'(b)/\chi(b)) = 0 \tag{8}$$

The Titchmarsh–Weyl m-function can be shown to be represented by a circle with an center C_b and a radius R_b as

$$C_b = -[\phi_\ell, \psi_\ell](b)/[\psi_\ell, \psi_\ell](b), \quad R_b = 1/[\psi_\ell, \psi_\ell](b)$$
$$\text{where } [f, g](t) = f(t)\bar{g}'(t) - f'(t)\bar{g}(t)$$

We now extend the boundary-value problem on a finite interval to an infinite interval by letting $b \to \infty$ along a path with a positive small imaginary part $\imath\epsilon$ and then let $\epsilon \to 0$. This implies that the radius will have two possible limits:

$$\Rightarrow R_b \to 0 \text{ (Limit point case)} \quad \text{or} \quad R_b \to R_\infty > 0 \text{ (Limit circle case)}. \tag{9}$$

Physics applications are of limit point type.

It can be shown that the Titchmarsh–Weyl function $m(E)$ is an analytic function of Nevanlinna type is related to the spectral function $\rho(\omega)$ such that for the wave function $\psi_\ell(\omega, r')$ we have

$$\text{completeness} : \delta(r - r') = \int_{-\infty}^{+\infty} \psi_\ell(\omega, r)\psi_\ell(\omega, r')d\rho(\omega)$$

$$\text{where} : \rho(\omega_1) - \rho(\omega_2) = \lim_{\epsilon\to 0^+} \frac{1}{\pi}\int_{\omega_1}^{\omega_2} \mathcal{I}m(m(\lambda + \imath\epsilon))d\lambda$$

$$\Rightarrow \text{yielding a definition of the Spectral density} : \mathcal{I}m(m(E)) = \pi\left(\frac{d\rho}{d\omega}\right)_{\omega=E} \tag{10}$$

The spectral function and the spectral density are illustrated in Fig. 1. Using Eq. (6) we can write the Titchmarsh–Weyl m-function as

$$m_{TW}(E) = \frac{W[\phi_\ell, \chi_\ell]}{W[\chi_\ell, \psi_\ell]}. \tag{11}$$

Thus $m_{TW}(E)$ can be evaluated from the logarithmic derivative χ'/χ.

Since m as well as χ have different properties dependent on $\Im(\lambda)$ we now need to define:

$$m(\lambda) = \begin{cases} m^+(\lambda);\ \Im(\lambda) > 0 \\ m^-(\lambda);\ \Im(\lambda) < 0 \end{cases} \quad \text{as well as} \quad \chi(\lambda) = \begin{cases} \chi^+(\lambda);\ \Im(\lambda) > 0 \\ \chi^-(\lambda);\ \Im(\lambda) < 0 \end{cases} \tag{12}$$

We will thus have

$$\chi_\ell^\pm(r) = \phi_\ell(r) + \psi_\ell(r)m^\pm(E) \tag{13}$$

2.3 Complex Scaling: a Brief Outline

In order to evaluate the quantities dependent on χ we will use the complex scaling method [3–8]. This theory states that if we analytically continue a Schrödinger problem H by scaling a radial coordinate r such that asymptotically

$$r \to r\exp(\imath\theta) \text{ as } r \to \infty \text{ when } 0 < \theta < \pi, \text{ such that } H(0) \to H(\theta) \tag{14}$$

we will find (1) that the bound spectrum of $H(\theta)$ will have the same as that of $H(0)$, (2) the continuous spectrum of $H(0)$ will be rotated down into the fourth quadrant of the complex energy plane by an angle -2θ and (3) a set of complex-valued discrete eigenvalues will appear in the uncovered sector defined by the angle $0 < \vartheta_{uncov} < -2\theta$.

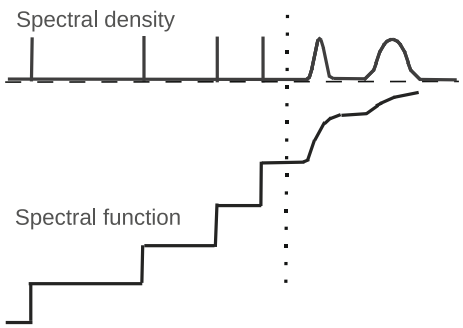

Fig. 1 Naive picture of spectral function, ρ and spectral density ($d\rho/d\omega$). The vertical positions of the spectral function and spectral density is arbitrary. The eigenenergies match. The *dotted vertical line* indicates the threshold. Below this threshold we have bound states and ρ is a step function at the bound states. Above the threshold we find more or less *sharp peaks* that correspond to the resonances

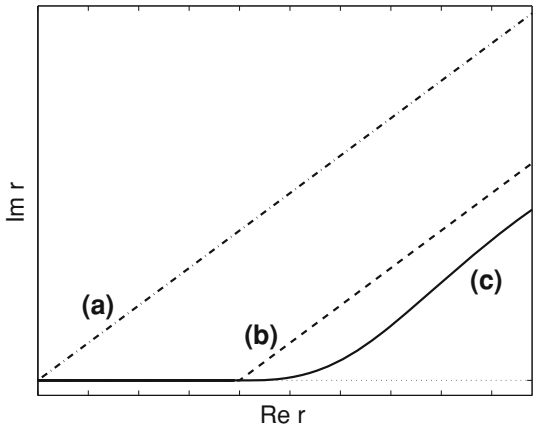

Fig. 2 **a** Uniform complex scaling, **b** sharp exterior scaling and **c** smooth exterior scaling

The so defined uniform complex scaling can be generalized to smooth exterior scaling [9] for instance through the transformation:

$$\xi(r) = \begin{cases} r, & r < r_0, \\ r + f(r, r_0, \theta, \rho), & r \geq r_0, \end{cases} \tag{15}$$

where

$$f(r, r_0, \theta, \rho) = (e^{i\theta} - 1)(r - r_0)(1 - \exp(-\rho(r - r_0)^2)). \tag{16}$$

This is illustrated in Fig. 2. For further use we now define $\eta = \exp(\imath\theta)$.

3 Resonances

Following the Aguilar–Balslev–Combes–Simon (ABCS) theory defines resonances for a Schrödinger operator H as the the set of poles to meromorphic continuations of all matrix elements of the resolvent of $H : R_H$ [10]. The ABCS theory can be applied to the Titchmarsh–Weyl theory by starting with

$$\left(-\frac{d^2}{dr^2} + \frac{\ell(\ell+1)}{r^2} + \eta^2 V_0(\eta r) - \eta^2\lambda\right) = 0 \tag{17}$$

The boundary conditions now take the form

$$\begin{pmatrix} \phi_{\ell,\eta} & \psi_{\ell,\eta} \\ \phi'_{\ell,\eta} & \psi'_{\ell,\eta} \end{pmatrix}_{r=a} = \begin{pmatrix} \sin\alpha & \cos\alpha \\ -\eta\cos\alpha & \eta\sin\alpha \end{pmatrix} \tag{18}$$

Provided the energy parameter is within an rotated, uncovered sector the dilated TW-circle still converges to a point(limit point case) as the scaled coordinate $|\eta r| \to \infty$.

Rewriting the dilated Schrödinger equation in terms of the logarithmic derivative $z_{\ell,\eta} = \chi'_{\ell,\eta}/\chi_{\ell,\eta}$ we get a complex dilated Riccati equation

$$z'_{\ell,\eta}(r) = 2\eta^2(V_0(\eta r) - \lambda) - z^2_{\ell,\eta} \tag{19}$$

From which the $m_{TW}(E)$ can be computed by analytical continuation, for example through complex scaling.

4 Generalized Spectral Expansion of the Green Function

4.1 Spectral Expansion Over Real Energy States

Consider the resolvent formulation of the Green function above written as

$$G^+(\lambda; r, r') = \lim_{\epsilon\to 0} \int_{-\infty}^{+\infty} \frac{d\hat{\tau}(\omega)}{\lambda + \imath\epsilon - \omega}$$

$$= \lim_{\epsilon\to 0} \left\{ \sum_j \frac{\mathcal{R}es[G^+(\lambda_j; r, r')]}{\lambda + \imath\epsilon - \lambda_j} + \int_0^{+\infty} \frac{[d\hat{\tau}/d\omega]d\omega}{\lambda + \imath\epsilon - \omega} \right\}_{\lambda\neq\lambda_j} \tag{20}$$

Extracting the imaginary part of the Green function (20) we find

$$\mathcal{I}m(G_\ell^+(\lambda; r, r')) = -\pi \left(\frac{d\hat{\tau}(\omega)}{d\omega}\right) = -\psi_\ell(r)\psi_\ell(r')\mathcal{I}m(m^+) \tag{21}$$

$$G_\ell^+(\lambda; r, r') = \lim_{\epsilon\to 0} \int_{-\infty}^{+\infty} ds \frac{\psi_\ell(\omega, r)\psi_\ell(\omega, r')d\rho(\omega)}{\lambda + \imath\epsilon - \omega} \tag{22}$$

with

$$\frac{d\rho(\omega)}{d\omega} = \begin{cases} \sum_j \dfrac{\delta(\omega - \lambda_j)}{< \psi_\ell(\lambda_j)|\psi_\ell(\lambda_j) >}; & \omega < 0 \\ \dfrac{1}{\pi}\mathcal{I}m(m^+(\omega)); & \omega > 0 \end{cases} \tag{23}$$

Letting the resolvent operator work on Eq. (22) one can show that the spectral densities (23) and (10) are the same. The Green function, in Eq. (22), above is thus uniquely defined by m_{TW}.

4.2 The Nevanlinna Representation of $m(E)$ and Its Extension

A Cauchy analytic function $f(z)$ is said to be of Nevanlinna type if it maps the upper (lower) complex half plane onto itself. It can be shown that $m(\lambda)$ is a function of Nevanlinna type. Nevanlinna functions posses a uniquely defined spectral functions $\sigma(\omega)$ such that

$$f(z) = \int_{-\infty}^{+\infty} \frac{d\sigma(\omega)}{\omega - z}; \tag{24}$$

$$\frac{d\sigma(\omega)}{d\omega} = \begin{cases} \sum_j -\mathcal{R}es[f(z_j)]\delta(\omega - z_j); \omega < 0 \\ \frac{1}{\pi}\mathcal{I}m(f(\omega + \imath 0)); \omega > 0 \end{cases}$$

Consider $\ell = 0$ only and let $m_{\text{free}} = \imath\sqrt{\lambda}$

$$\Rightarrow \; m(\lambda) - \imath\sqrt{\lambda} = \int_{-\infty}^{+\infty} \frac{d\sigma(\omega)}{\omega - z}; \; d\sigma(\omega) = d\rho(\omega) - d\rho_{\text{free}}(\omega) \tag{25}$$

Now make a complex dilation of χ and m defined in Eq. (12)

First we note that the rotated cut now can be described through $\eta^{-2}R^+$. This implies that

$$m_\eta(\lambda) = \begin{cases} m_\eta^+(\lambda); \; \Im(\eta^2\lambda) > 0 \\ m_\eta^-(\lambda); \; \Im(\eta^2\lambda) < 0 \end{cases}; \quad \chi_\eta(\lambda) = \begin{cases} \chi_\eta^+(\lambda); \; \Im(\eta^2\lambda) > 0 \\ \chi_\eta^-(\lambda); \; \Im(\eta^2\lambda) < 0 \end{cases} \tag{26}$$

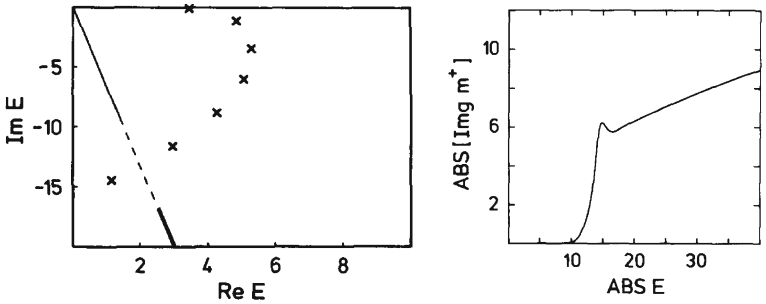

Fig. 3 *Left figure* Pole string for $m^+(\lambda)$, $\lambda = 2E$. The ray $\eta^{-2}R^+$ displays the integration contour for the Nevanlinna representation. *Right figure* The generalized spectral density is vanishingly small along the *weakly drawn line*. Outside, along the *thick solid line* the generalized spectral density is that of a free particle. The *broken line* shows the transition region (from ref. [2])

Above we defined $m^+(\lambda)$ and $m^-(\lambda)$ to have analytic continuation onto higher Riemann sheets. It can be shown that for real λ they differ only by the signs of their imaginary parts

$$\mathcal{I}m(m^+(\lambda)) = (m^+(\lambda) - m^-(\lambda))/2\imath \equiv \mathcal{I}mg(m(\lambda)) \tag{27}$$

thereby defining $\mathcal{I}mg(m(\lambda))$.

$$\Rightarrow m^+(\lambda) - \imath\sqrt{\lambda} = \sum_j \frac{\mathcal{R}es[m^+(\lambda_j)]}{\lambda - \lambda_j} + \int_C \frac{\mathcal{I}mg(m^+(\omega) - \imath\sqrt{\omega})d\omega}{\omega - \lambda} \tag{28}$$

where C is the rotated continuum defined in Sect. 2.3. We thus find

$$\frac{d\rho(\omega)}{d\omega} = \frac{1}{\pi}\mathcal{I}mg(m^+(\omega)) \tag{29}$$

The implication of Eq. (28) is illustrated in Fig. 3, namely since the spectral density additive and can be constructed from the individual contributions from the poles of the Titchmarsh–Weyl m-function by adding to this sum the contribution form the free particle m-function : $m_{free} = \imath\sqrt{\lambda}$. Having reviewed the structure of the eigenvalue spectrum of a two-body Schrödinger Hamiltonian we now turn to what implication this spectrum may have on the understanding of a scattering problem.

5 Two-Channel Scattering Problem and how it Can Be Analyzed in Terms of the Spectrum of the Associated Schrödinger Hamiltonian

The careful, curious reader can find the details of the results presented here in ref. [11–13]. Consider a scattering process that can be described as a two-channel Schrödinger problem

$$\begin{aligned}\left(-\frac{d^2}{dr^2} + U_{11} + \frac{\ell(\ell+1)}{r^2} - k_1^2\right)\phi_1(r) + U_{12}\phi_2(r) = 0,\\ \left(-\frac{d^2}{dr^2} + U_{22} + \frac{\ell(\ell+1)}{r^2} - k_2^2\right)\phi_2(r) + U_{21}\phi_1(r) = 0,\end{aligned} \tag{30}$$

where ℓ is the angular momentum quantum number.

$$k_n = \sqrt{2m(E - E_n)} \tag{31}$$

is the channel momentum while E_n denotes the channel threshold and m is the reduced mass of the studied system. The scattering is described by the Scattering Operator $\hat{S}$ acting on the incoming wave Ψ_{in} to give the outgoing wave Ψ_{out}

$$\Psi_{out} = \hat{S}\Psi_{in} \tag{32}$$

For a central potentials $U(\mathbf{r}) = U(r)$ we formulate the problem in terms of an expectation value problem: the partial wave scattering matrix $S_{\ell,ij}(E)$ yielding the total cross section in terms of the partial wave scattering cross sections

$$\sigma_{ij}(E) = \sum_{\ell=0}^{\infty} \sigma_{\ell,ij}(E); \quad \sigma_{\ell,ij}(E) = 4\pi(2\ell+1)\left|\frac{S_{\ell,ij}(E) - \delta_{ij}}{2\imath k_i}\right|^2 \tag{33}$$

The Mittag-Leffler (ML) expansion of the S-matrix, being a meromorphic function, is given by:

$$S(k) = S(a) + \sum_R Res\left[S(z_R)\right]\left\{\frac{1}{k - z_R} + \frac{1}{z_R - a}\right\} + \frac{k-a}{2\pi i}\oint\limits_C \frac{S(z)\,dz}{(z-k)(z-a)}. \tag{34}$$

where the contour C follows the inside of the rotated continuum $-\eta^2 R^+$ out to infinity, then along a sector with infinite radius and back to the lowest threshold along $\eta^2 R^+$.

5.1 The Many Channel Partial Wave S-Matrix and Its Residues at Resonant Energies

Here and below matrices are labeled with fat symbols. The many-channel partial wave S-matrix can be expressed as

$$\mathbf{S}_\ell = \mathbf{1} + 2i\mathbf{K}^{1/2}\mathbf{F}_\ell\mathbf{K}^{1/2}, \text{ where } \mathbf{K} = \begin{bmatrix} k_1 & 0 \\ 0 & k_2 \end{bmatrix}. \tag{35}$$

where $\mathbf{K}$ is the (here two-channel) momentum matrix and $\mathbf{F}_\ell$ is the scattering amplitude (proportional to the T-matrix elements)

$$\mathbf{F}_\ell = -\mathbf{K}^{-1}\int\limits_0^\infty dr\,\hat{\mathbf{j}}_\ell(\mathbf{K}r)\mathbf{U}(r)\Psi_\ell(r)\mathbf{K}^{-1}. \tag{36}$$

Here $\hat{\mathbf{j}}_\ell(\mathbf{K}r)$ is a diagonal matrix of the Riccati-Bessel functions, $\mathbf{U}(r)$ - potential matrix and $\Psi_\ell(r)$ is a physical solution of Schrödinger Eq. (30) which also satisfies the integral equation

$$\Psi_\ell(r) = \hat{\mathbf{j}}_\ell(\mathbf{K}r) + \int\limits_0^\infty dr'\,\mathbf{G}(r,r')\mathbf{U}(r')\hat{\mathbf{j}}_\ell(\mathbf{K}r'). \tag{37}$$

Each column in the matrix $\Psi_\ell(r)$ is a solution to the Schrödinger equation with appropriate boundary conditions.

The two-channel partial wave Green function is expressed in its eigenfunctions. Then, by applying complex dilation to the Green function and discretizing the contributions from the continuous spectrum, the complex dilated two-channel partial Green function is obtained as a finite sum over the eigenfunctions

$$\mathbf{G}(r,r') = \sum_{R=1}^{N}\frac{1}{E - E_R}\begin{bmatrix}\phi_1^R(r) \\ \phi_2^R(r)\end{bmatrix}\left[\phi_1^R(r'),\,\phi_2^R(r')\right]. \tag{38}$$

Substituting (36)–(38) into Eq. (35), the following expression for the S-matrix is obtained

$$\mathbf{S}_\ell = 1 - 2i\mathbf{K}^{-1/2}\int\limits_0^\infty dr\,\hat{\mathbf{j}}_\ell(\mathbf{K}r)\mathbf{U}(r)\hat{\mathbf{j}}_\ell(\mathbf{K}r)\mathbf{K}^{-1/2} \tag{39}$$

$$-\mathbf{K}^{-1/2}\sum_{R=1}^{N}\frac{2i}{E - E_R}\int\limits_0^{\xi(\infty)} d\xi(r)\,\hat{\mathbf{j}}_\ell(\mathbf{K}\xi(r))\mathbf{U}(\xi(r))\phi_R(\xi(r)) * \tag{40}$$

$$\int\limits_0^{\xi(\infty)} d\xi(r)\,\phi_R^T(\xi(r))\mathbf{U}(\xi(r))\hat{\mathbf{j}}_\ell(\mathbf{K}\xi(r))\mathbf{K}^{-1/2}. \tag{41}$$

Yielding the residue of the S-matrix at a resonance momentum

$$Res\left[\mathbf{S}_\ell(\mathbf{K}_R)\right] = -i\mathbf{K}_R^{-1} \int_0^{\xi(\infty)} d\xi(r)\, \mathbf{K}_R^{-1/2} \hat{\mathbf{j}}_\ell(\mathbf{K}_R\xi(r))\mathbf{U}(\xi(r))\phi_R(\xi(r)) * \tag{42}$$

$$\int_0^{\xi(\infty)} d\xi(r)\, \phi_R^T(\xi(r))\mathbf{U}(\xi(r))\hat{\mathbf{j}}_\ell(\mathbf{K}_R\xi(r))\mathbf{K}_R^{-1/2}. \tag{43}$$

The contribution to partial wave S-matrix a single resonance is defined as the residue term in the ML expansion:

$$Res\left[\mathbf{S}_\ell(\mathbf{K}_R)\right](\mathbf{K}-\mathbf{K}_R)^{-1} \tag{44}$$

$\mathbf{K}_R$ is defined in the same way and is the momentum matrix at the resonance energy. The residues of the S-matrix can then be calculated and used to define and build the reduced S-matrix, $\tilde{\mathbf{S}}_\ell(\mathbf{K}, \mathbf{K}_R)$:

$$\tilde{\mathbf{S}}_\ell(\mathbf{K}, \mathbf{K}_R) = \mathbf{S}_\ell(\mathbf{K}) - Res\left[\mathbf{S}_\ell(\mathbf{K}_R)\right](\mathbf{K}-\mathbf{K}_R)^{-1}. \tag{45}$$

The reduced partial cross section is then given by

$$\tilde{\sigma}_{\ell,ij}(E, E_R) = 4\pi(2\ell+1)\left|\frac{\tilde{S}_{\ell,ij} - \delta_{ij}}{2\imath k_i}\right|^2. \tag{46}$$

The difference between σ_ℓ and $\tilde{\sigma}_\ell$ can then be used to identify a possible feature in the cross section.

5.2 The Noro–Taylor Potential as a Numerical Example

The Noro–Taylor potential [14] in our example is

$$\mathbf{V}(r) = \begin{bmatrix} -1.0 & -7.5 \\ -7.5 & 7.5 \end{bmatrix} r^2 e^{-r}, \tag{47}$$

where the threshold energies are $E_1 = 0$ and $E_2 = 0.1$, respectively. As in the previous sections, the notation $U(r) = 2mV(r),\ m = 1$ is used.

5.3 Resonance Energies, Their S-Matrix Residues and Their Influence on the Cross Section

Figure 4 illustrates the begin of the set of eigenvalues associated with the Noro–Taylor potential. Note that these resonances seem all to lay on trajectories. The real part of the eigen energy first increases with the resonance number, then reaches a maximum and finally move out in the complex energy plane. Studies have shown that they even can have negative real energies. The imaginary part of the resonances increase with the resonance number. The different angular momentum trajectories are quite close to each other. This behaviour, originally studied numerically [15,16] has been rigorously analyzed [17] in terms of bounds on complex eigenvalues and resonances. A string of partial wave S-matrix residues also appear in a regular pattern as shown in Fig. 5. The residues rotate anti-clockwise as the resonance number increases. $|Res(S_{\ell,ij}(E_R)|$ grows along the string of resonances implying that the common statement **"A wide resonance does not influence the cross section since it is so far out in the complex plane" is wrong.** Let us now turn to the corresponding cross sections. Figure 6 illustrates the influence of the first and the second resonance for the Noro–Taylor problem.

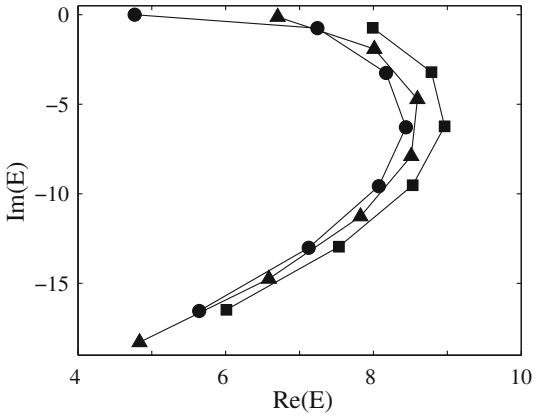

Fig. 4 Complex eigenvalues for the Noro–Taylor potential. Energies for $\ell = 0$ are marked with *filled circles*, for $\ell = 1$ and $\ell = 2$ with *filled triangles* and *squares*, respectively (from ref. [12])

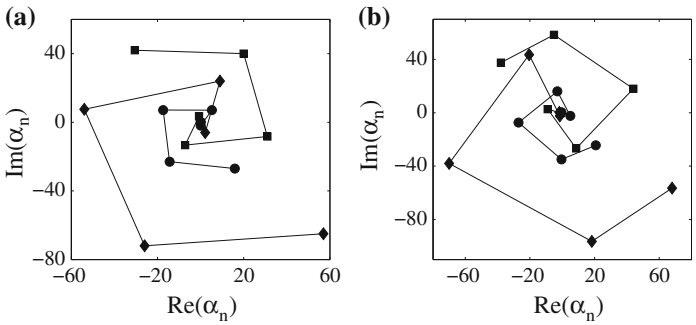

Fig. 5 Residues of the partial wave S-matrix elements **a** $\ell = 1$ and **b** $\ell = 2$. *Filled circles* correspond to the residues of S_{11}, *squares* and *diamonds* to the residues of S_{12} and S_{22} respectively. $\alpha_n = Res\left[S_{ij}(E_n)\right]$ (from ref. [12])

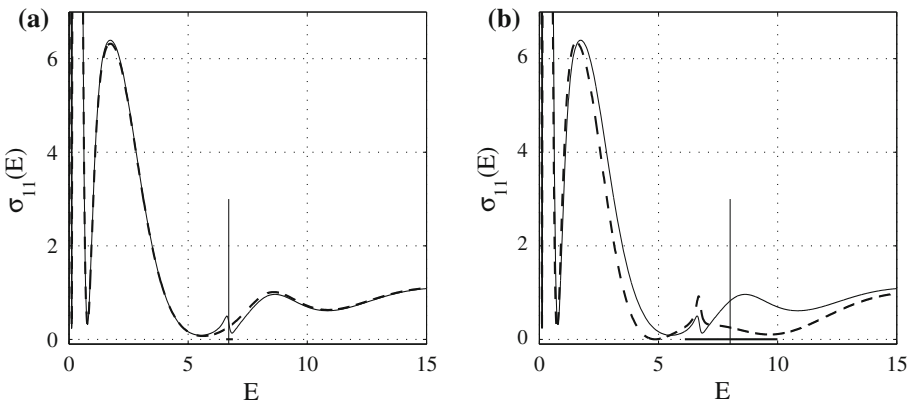

Fig. 6 σ_{11} cross sections for $\ell = 1$. *Solid line* corresponds to the partial wave cross section, *dashed line* corresponds to the reduced cross section based on Eq. (46) without contribution from **a** the first pole **b** the second pole. *Vertical lines* indicate positions of the excluded resonances, *horizontal lines* show intervals corresponding to the resonance width (from ref. [12])

5.3.1 The Breit–Wigner Approximation

A critical reader may argue that this the influence of of a resonance on the cross section was formulated by Breit and Wigner [18]. The Breit–Wigner (BW) formula for the partial wave S-matrix in the neighborhood of an isolated multichannel resonance, with a complex energy E_R, is given by

$$S_{ij}^{BW}(E, E_R) = \exp(2i\gamma_i)\delta_{ij} - i\exp(i(\gamma_i + \gamma_j))\frac{\sqrt{\Gamma_i\Gamma_j}}{E - E_R}, \tag{48}$$

yielding the BW residue as

$$-i\exp(i(\gamma_i+\gamma_j))\sqrt{\Gamma_i\Gamma_j}.$$

Here γ_i is a background phase shift and Γ_i is the corresponding partial width. One obvious problem with Breit–Wigner partial wave S-matrix is that it includes unknown values, namely the background phase shifts γ_i. It is unclear how this phase shifts are to be determined. We have here chosen to calculate them such that in a close vicinity of a resonance ($\mathrm{Re}(E_R)$) a partial wave S-matrix element $S_{ij}(E)$, obtained with the logarithmic derivative method, is equal to $S_{ij}^{BW}(E,E_R)$ in Eq. (48). We may now define a reduced BW partial-wave S-matrix, as

$$\tilde{S}_{ij}^{BW}(E,E_R)=S_{ij}(E)+i\exp(i(\gamma_i+\gamma_j))\frac{\sqrt{\Gamma_i\Gamma_j}}{E-E_R}. \tag{49}$$

Then we can define a BW reduced cross section as

$$\tilde{\sigma}_{ij}^{BW}(E,E_R)=4\pi(2\ell+1)\left|\frac{\tilde{S}_{ij}^{BW}(E,E_R)-\delta_{ij}}{2\imath k_i}\right|^2. \tag{50}$$

Figure 7 illustrates the difference between the reduced S-matrix and the Breit–Wigner approaches. Even though the difference between the two may be small we see in Fig. 7b that the improper Breit–Wigner description may indicate a false, second resonance which is not present in the reduced S-matrix analysis.

From this we may conclude that the Mittag-Leffler based S-matrix residue description of the resonance contribution to the studied cross sections is successful. The background phase in the Breit–Wigner varies even over a narrow resonance leaving a contribution from the resonance pole.

6 Summary

Our message to the participants of meetings at which this review was presented can be summarized as:

- Scattering resonances in the Schrödinger sense are mathematically rigorously defined as poles of the meromorphically continued resolvent of the corresponding Schrödinger Hamiltonian.
- The resonance poles associated with a potential or a set of coupled potentials form strings in the complex energy plane. Only certain areas in the complex energy plane can have resonances.
- The spectral density can be partitioned into contributions from the resonances and the free particle spectral density.
- The contributions form resonances to the scattering cross section can be formulated in terms of the S-matrix residues of resonances energies.

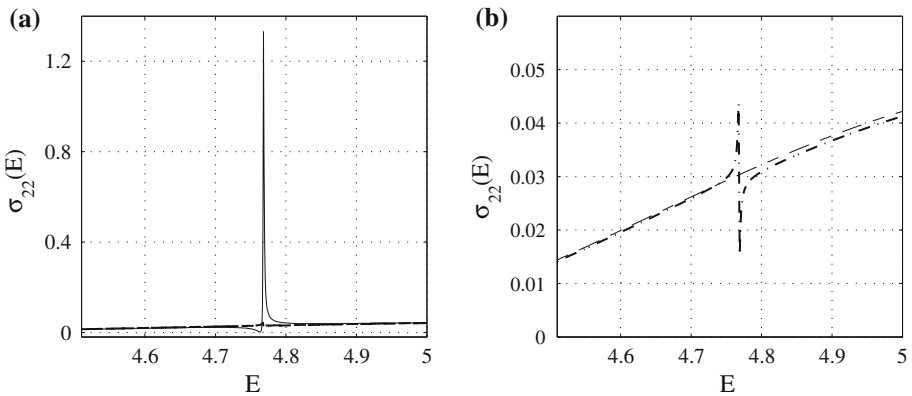

Fig. 7 σ_{22} cross sections for $\ell=0$. In **a** *solid line* corresponds to the partial wave cross section, the *dashed line* corresponds to the reduced cross section based on subtracting S-matrix residue from the first pole [Eq. (46)]. **b** The *dash-dotted line* reveres to the Breit–Wigner based reduced cross section [Eq. (50)] without contribution from the first pole while the *dashed line* has the same meaning as in **a** (from ref. [12])

- The S-matrix residues "rotate" anti-clockwise as n increases. $|Res(S_{\ell,ij}(E_R)|$ grows along the string of resonances $\Rightarrow$ the common statement **"A wide resonance does not influence the cross section since it is so far out in the complex plane" is wrong.**
- The Mittag-Leffler based S-matrix residue description of the resonance contribution to the studied cross sections is successful. The background phase in the Breit–Wigner varies even over a narrow resonance leaving a contribution from the resonance pole.

Acknowledgements This report was presented at the workshop on Critical Stability in Erice held during the week 9–15 October 2011. Both authors want to thank the organizers for inviting us. A similar presentation was given in honor of Erik Balslev at his 75th birthday workshop in September 2010. This work is supported by Swedish Research Council as well as the Swedish International Development Cooperation Agency (SIDA) and the National Research Foundation of South Africa.

References

1. Coddinton, E.A., Levinson, N.A.: Theory of ordinary differential equations. McGrraw-Hill Book Company, New York (1955)
2. Engdahl, E., Brändas, E., Rittby, M., Elander, N.: Generalized Green-functions and spectral densities in the complex energy plane. J. Math. Phys. **27**, 2629 (1986)
3. Aguilar, J., Combes, J.M.: Class of analytic perturbations for one-body Schrödinger Hamiltonians. Commun. Math. Phys. **22**, 269 (1971)
4. Balslev, E., Combes, J.M.: Spectral properties of many-body Schrödinger operators with dilation-analytic interactions. Commun. Math. Phys. **22**, 280 (1971)
5. Simon, B.: Resonances in body quantum systems with dilatation analytic potentials and foundations of time-dependent perturbation-theory. Ann. Math. **97**, 247 (1973)
6. van Winter, C.: Complex dynamical variables for multiparticle systems with analytic interactions.1. J. Math. Anal. Appl. **47**, 633 (1974)
7. van Winter, C.: Complex dynamical variables for multiparticle systems with analytic interactions.2. J. Math. Anal. Appl. **48**, 368 (1974)
8. Simon, B.: Definition of molecular resonance curves by the method of exterior complex scaling. Phys. Lett. A **71**, 211 (1979)
9. Elander, N., Levin, S., Yarevsky, E.: Full-angular-momentum, three-dimensional, smooth exterior complex dilated, finite-element method for computing resonances in triatomic molecules. Application to a model of the NeICl van der Waals complex. Phys. Rev. A **64**, 12505 (2001)
10. Hislop, P.D., Sigal, I.M.:Introduction to spectral theory with application to Schrödinger operators. In: Applied mathematical science, vol. 113. Springer, New York (1996)
11. Rakityansky, S.A., Elander, N.: Analyzing the contribution of individual resonance poles of the S-matrix to the two-channel scattering. Int. J. Quantum Chem. **109**, 1105 (2006)
12. Shilyaeva, K., Elander, N., Yarevsky, E.: The role of resonances in building cross sections: the Mittag-Leffler expansion in a two-channel scattering. Int. J. Quantum Chem. **109**, 414 (2009)
13. Shilyaeva, K., Elander, N., Yarevsky, E.: Identifying resonance structures in a scattering cross section using the $N^{3+} + H \rightarrow NH^{3+} \rightarrow N^{2+} + H^{+}$ reaction as an example. J. Phys. B **42**, 044011 (2009)
14. Noro, T., Taylor, H.S.: Resonance partial widths and partial photodetachment rate using the rotated-coordinate method. J. Phys. B **13**, L377 (1980)
15. Rittby, M., Elander, N., Brändas, E.: Weyl's theory and the method of complex rotation. A synthesis for a description of the continuous spectrum. Mol. Phys. **45**, 553 (1982)
16. Rittby, M., Elander, N., Brändas, E.: Reply to a comment on Weyl's theory and the complex rotation method applied to phenomena associated with a continuous spectrum. Phys. Rev. A **26**, 1804 (1982)
17. Abramov, A.A., Aslanyan, A., Davies, E.B.: Bounds on complex eigenvalues and resonances. J. Phys. A Math. Gen. **34**, 57 (2001)
18. Breit, G., Wigner, E.: Capture of slow neutrons. Phys. Rev. A **49**, 519 (1936)